

Volume 95 Number 10 October 2014

BAMS




Bulletin of the American Meteorological Society

MOORE EF5 TORNADO ANALYZED

FIELD WORK FOR UNDERGRADUATES

LAND-CHANGE EFFECTS ON CLIMATE



**Deep Questions
in Shallow Water**
The Taihu Eddy Flux Network

THE TAIHU EDDY FLUX NETWORK

An Observational Program on Energy, Water, and Greenhouse Gas Fluxes of a Large Freshwater Lake

BY XUHUI LEE, SHOUDONG LIU, WEI XIAO, WEI WANG, ZHIQIU GAO, CHANG CAO, CHENG HU, ZHENGHUA HU, SHUANGHE SHEN, YONGWEI WANG, XUEFA WEN, QITAO XIAO, JIAPING XU, JINBIAO YANG, AND MI ZHANG

In situ eddy covariance observations reveal unusually large nocturnal CO₂ uptake by submerged vegetation in a shallow lake.

MOTIVATION AND SCIENCE QUESTIONS.

Lakes are an important component of the climate system. Even though lakes and reservoirs occupy only about 4% of the global terrestrial surface (Downing et al. 2006), their societal importance is disproportionately large because many large municipalities are located near lake shorelines. The large thermal contrast between a lake and its surrounding land often triggers thermal circulations, having significant impact on air pollution dispersion and transport in the lake catchment. Being important sources of atmospheric moisture, large lakes can enhance storm formation in the downwind area (Samuelsson et al. 2010; Zhao et al. 2012). Except at times of high algal

activities (Hari et al. 2008; Balmer and Downing 2011), lake water is usually supersaturated in CO₂ with respect to the atmosphere and acts as a source of atmospheric carbon (Cole et al. 1994). Lakes are also sources of atmospheric CH₄ (Bastviken et al. 2011) and N₂O (Huttunen et al. 2003).

Eddy covariance (EC) is an in situ technique for measuring momentum, heat, water, and greenhouse gas fluxes. It determines the flux continuously and nonintrusively from simultaneous measurements, in the atmospheric surface layer, of turbulent fluctuations in the air velocity and the scalar quantity of interest. The method is a key measurement tool deployed by several large observational networks,

AFFILIATIONS: LEE—Yale—NUIST Center on Atmospheric Environment, Nanjing University of Information, Science and Technology, Nanjing, China, and School of Forestry and Environmental Studies, Yale University, New Haven, Connecticut; LIU, W. XIAO, W. WANG, CAO, HU, Y. WANG, Q. XIAO, XU, AND ZHANG—Yale—NUIST Center on Atmospheric Environment, Nanjing University of Information, Science and Technology, Nanjing, China; GAO—Yale—NUIST Center on Atmospheric Environment, and College of Applied Meteorology, Nanjing University of Information, Science and Technology, Nanjing, China; SHEN—College of Applied Meteorology, Nanjing University of Information, Science and Technology, Nanjing, China; WEN—Key Laboratory of Ecosystem Network Observation and Modeling, Institute of

Geographic Sciences and Natural Resources Research, Chinese Academy of Sciences, Beijing, China; YANG—Suzhou Meteorological Bureau, Suzhou, China

CORRESPONDING AUTHOR: Xuhui Lee, School of Forestry and Environmental Studies, Yale University, New Haven, CT 06511
E-mail: xuhui.lee@yale.edu

The abstract for this article can be found in this issue, following the table of contents.

DOI:10.1175/BAMS-D-13-00136.1

A supplement to this article is available online (10.1175/BAMS-D-13-00136.2)

In final form 30 April 2014
©2014 American Meteorological Society

such as the Global Flux Network (FLUXNET; Baldocchi et al. 2001), the National Ecological Observatory Network in the United States (Schimel et al. 2007), and the Integrated Carbon Observation System in Europe (www.icos-infrastructure.eu). These networks are playing increasingly important roles in Earth and ecological sciences. Most of the EC sites in these networks are located in upland ecosystems. Owing to logistical difficulties, long-term (>1 yr) EC applications are still rare for lake systems (Rouse et al. 2008; Blanken et al. 2011; Nordbo et al. 2011; Liu et al. 2012). The water equilibrium method and floating chambers, two traditional methods for measuring lake–air gaseous fluxes, are suitable for short field campaigns but are difficult to deploy in uninterrupted long-term operations (St. Louis et al. 2000; Schubert et al. 2012). In addition, they cannot measure energy, momentum, and water fluxes, and yet these fluxes are the primary drivers of the physical state of the atmosphere and the lake system.

Imbedded in the above regional and global networks are a number of small EC clusters. By design, sites in these clusters are positioned in close

proximity, usually within tens of kilometers from one another, and are influenced by nearly identical climate conditions. The observed spatial variations reveal gradient effects of land management (Zha et al. 2009; Prescher et al. 2010), ecological succession (Stoy et al. 2008), and natural disturbance (Goulden et al. 2006; Brown et al. 2012). Here we adopt the same research strategy to monitor the temporal and spatial patterns of lake–air fluxes.

In this article, we describe an EC network on Lake Taihu, a large and shallow lake in southeastern China. Globally, 28% of inland lakes are shallow (depth < 5 m) according to the Global Lake Database (www.flake.igb-berlin.de/ep-data.shtml). The network consists of five lake sites, representing different biological attributes, pollution status, and wind–wave patterns, and a land site near the lake shore. Lake Taihu is an environmental hot spot. It is located in the Yangtze River Delta and is the third largest freshwater lake in China. The lake basin is heavily urbanized, with five large municipalities (each with populations greater than one million) situated near the lake shoreline. Frequent algal blooms and air quality problems in recent years have spurred considerable interest among scientists and decision makers in processes governing the lake–atmosphere interactions.

Our study appears to represent the first lake EC network. Our goal is to quantify the lake–air fluxes of energy, momentum, and greenhouse gases across pollution and biological gradients in the lake. The data will be used to address five science questions:

- 1) Are lake–air parameterizations established for deep lakes applicable to shallow lakes?
- 2) Why are lake–land breeze circulations less prevalent in the Taihu lake basin than in lake basins in northern latitudes?
- 3) How do algal blooms alter the lake–atmosphere interactions?
- 4) Is this eutrophic lake a source or sink of atmospheric CO_2 ?
- 5) Does the decay of algal and macrophyte biomass contribute significant amounts of CH_4 to the atmosphere?

The objective of this paper is to provide an overview of this field program. To date, some progress has been made toward answering the first science question, using data from a subset of the eddy flux sites (Deng et al. 2013; Xiao et al. 2013; Wang et al. 2014). A brief summary of the results is given below. In addition, we describe an unusual phenomenon of large nocturnal CO_2 uptake by submerged vegetation in the lake.

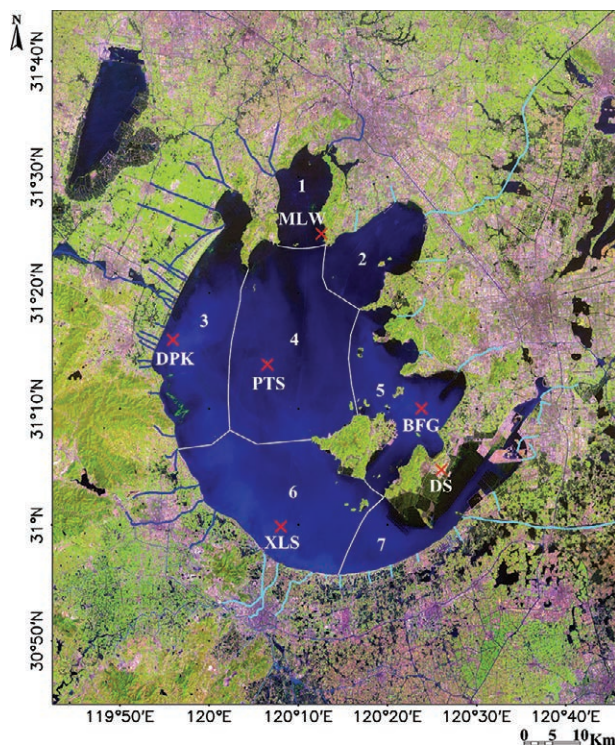


FIG. 1. A *Landsat 8* image of Lake Taihu and its surrounding area, taken on 14 Apr 2013. Color composite is 654 red-blue-green (RGB). Red crosses mark locations of the eddy covariance sites. Blue and green lines mark inflow and outflow rivers, respectively. Areas in green are vegetation and areas in purple and brown are cities.

SITE DESCRIPTION.

The Lake Taihu catchment belongs to four administrative units: Jiangsu Province, Zhejiang Province, Anhui Province, and Shanghai Municipality. To the north and east of the lake are floodplains with an elevation range of 4–6 m and to the west are highlands with elevation of 10–1250 m. The lake itself is situated at 30°5'40"–31°32'58"N, 119°52'32"–120°36'10"E, with a total area of approximately 2400 km² (Fig. 1). A reference map is given by Xiao et al. (2013). The lake has a mean depth of 1.9 m, with the northern and western portions being deeper (depth 2.5 m) and eastern portion shallower (depth <1.5 m; Qin et al. 2007). The lake bottom has an average elevation of 1.1 m above mean sea level. According to spatial variations of pollution loading (Zhao et al. 2011), vegetation abundance (Liu et al. 2007), and wind–current interaction (Qin et al. 2007), the lake is now divided into seven biophysically distinct zones (Fig. 1; Hu et al. 2011). Zone 1 is a semi-enclosed bay. It has low wind speed and nearly stagnant water, and is eutrophic. Zone 2 is connected to one of the largest outflow waterways, with half of the water covered by floating plants and emergent macrophytes. Receiving large quantities of nutrients from the inflow rivers, Zone 3 is hypereutrophic. Zone 4 in the center of the lake has relatively low photosynthetic activity. Zone 5 is dominated by submerged macrophytes, zone 6 represents a transition between phytoplankton dominance and macrophyte dominance, and zone 7 is characterized by submerged macrophytes and pen fish farming.

Table 1 lists a few key climate variables. The climate in the lake catchment is humid-subtropical according to the Köppen climate classification. Water flows into the lake through 27 rivers and canals connected to the west and north shores and outflow water leaves the lake through 22 waterways connected to the east shore. The annual mean flow is about 88×10^8 m³ (Yan et al. 2011). In some of the rivers, flow reversal can occur at times of low water level in the summer. The mean residence time of the lake water is about 350 days (An and Wang 2008).

In recent decades, rapid urbanization and intensification of industry in the lake catchment have caused severe environmental pollution. The lake total nitrogen concentration increased from the pre-1980 level of 0.05 mg L⁻¹ to 1.97 mg L⁻¹ in 2012 (An and

TABLE 1. Climate variables and energy balance components at Lake Taihu. Climate variables are for 1981–2010 measured at the Wuxi surface weather station near the north shore of the lake. Energy flux components are for year 2011 measured at MLW in the lake and are averaged over 24-h period of the day (Fig. 1).

Climatology		Energy flux (W m ⁻²)	
Air temperature (°C)	16.2	Incoming solar radiation	143.8
Annual precipitation (mm)	1122	Net radiation	87.1
Wind speed (m s ⁻¹)	2.6	Sensible heat flux	9.8
Dewpoint temperature (°C)	14.1	Latent heat flux	77.3

Wang 2008; Taihu Office 2013). Frequent algal blooms (see supplementary Fig. ES1; supplementary data are available online at <http://dx.doi.org/10.1175/BAMS-D-13-00136.2>) have altered the biophysical characteristics of the lake system and have threatened the water supply to several large cities in the lake catchment (Zhang et al. 2010).

Local air quality has also deteriorated. According to the data provided by the Suzhou Meteorological Bureau, the 2012 annual mean PM_{2.5} concentration in Suzhou City is 43 μg m⁻³, with the daily mean reaching as high as 150 μg m⁻³, far exceeding the U.S. Environmental Protection Agency air quality annual limit of 15 μg m⁻³ and daily limit of 35 μg m⁻³. Generally, cities at the shoreline of a large lake should have good air quality because of favorable dispersion conditions associated with lake breeze circulations. But this is not the case for Suzhou and other cities near Lake Taihu. Using the detection method described by Sills et al. (2011), we found that the frequency of lake breeze occurrence is about 20% in the summer of 2012, much lower than that reported for the southern Great Lakes region (76% in June–August 2007; Sills et al. 2011). Concurrent energy flux measurements on land and in the lake will provide critical data input to mesoscale models to determine whether the low occurrence frequency is intrinsic to shallow lake systems in subtropical latitudes.

RESEARCH DESIGN. Eddy covariance. The field experiment addresses science questions 3–5. Currently, the Lake Taihu Eddy Flux Network consists of five lake sites and one land site (Fig. 1; Table 2). Common to these sites are an EC system consisting of a sonic anemometer/thermometer (model CSAT3, Campbell Scientific Inc., Logan, Utah) and an open-path H₂O/CO₂ analyzer (Table 2), a four-way net radiometer (model CNR4, Kipp & Zonen B. V., Delft, the Netherlands), an anemometer and wind vane (model 05103; R M Young Company, Traverse

City, Michigan), and an air temperature and humidity probe (model HMP155A; Vaisala, Inc., Helsinki, Finland). At the lake sites, water temperature is measured at depths of 0.20, 0.50, 1.00, and 1.50 m, and sediment temperature at the depth of ~0.10 m below the water column (temperature probes model 109-L, Campbell Scientific). At the land site, soil temperature is measured at depths of 0.05, 0.10, and 0.20 m (temperature probes model 109-L, Campbell Scientific) and soil heat flux at the depth of 0.05 and 0.10 m (heat flux plate model HFP01SC; Hukseflux Thermal Sensors B. V., Delft, the Netherlands). At the MLW lake site, the sensors are mounted on small (diameter 30 cm) concrete pillars and connected to A/C power. At the other four lake sites (DPK, BFG, PTS, XLS; see Table 2), the sensors are mounted on an in-lake platform (dimension 3–5 m) and powered by an array of solar panels (Fig. 2). The EC signals are recorded at 10 Hz by a datalogger (model CR 3000, Campbell Scientific), which also performs online flux computation using the block averaging procedure (Lee et al. 2004). All other variables are sampled at 1 Hz by another datalogger (model CR1000, Campbell Scientific).

The prevailing wind is southeast in the summer and northeast in the winter. Wind speed varies among the lake sites. Having more open fetch, PTS and DPK are windier than the other sites. The 10-m mean wind speed for the period July–September 2013 is 3.6 m s⁻¹ at MLW, 4.8 m s⁻¹ at DPK, 5.0 m s⁻¹ at BFG, 4.7 m s⁻¹ at XLS, and 5.0 m s⁻¹ at PTS. A footprint analysis for MLW, DPK, and BFG is given by Wang et al. (2014).

Two lake sites (MLW and BFG) have enhanced measurement capacity. MLW is a supersite located in the Meiliangwan Bay. A 250-m-long boardwalk

provides easy access to the instruments. A small raised instrument shed at the end of the boardwalk houses two laser-based analyzers for simultaneous measurement of CO₂, CH₄, and H₂O mixing ratios (Model G1301, Picarro Inc., Santa Clara, California) and for measurement of the D and ¹⁸O isotopic compositions of water vapor (model DLT-100, Los Gatos Research, Mountain View, California). These analyzers are configured in gradient mode, switching every 30–60 s between air samples drawn from the heights of 1.1 and 3.5 m above the water surface. The fluxes of H₂O, CO₂, and CH₄ and the isotopic compositions of lake evaporation are determined with the gradient-diffusion method. Water samples are collected daily at midday from the 20-cm depth for analysis of pH, D, and ¹⁸O isotopic compositions and dissolved CO₂, CH₄, and N₂O concentrations. Water chemical parameters (pH, turbidity, dissolved oxygen, chlorophyll, blue-green algae phycocyanin, conductivity, salinity, oxidation reduction potential) are recorded every 15 min by an early warning monitoring system (model GuardianBlue, HACH Company, Loveland, Colorado) and a multi-parameter water quality analyzer (model YSI6600, YSI Inc., Yellow Spring, Ohio).

At the BFG site, the dissolved oxygen content, oxidation reduction potential, water temperature, conductivity, and pH are monitored continuously (model Professional Plus, YSI Inc.). A T-chain (PME Inc., Vista, California) provides another set of water temperature profile measurements. A second eddy covariance system, consisting of a sonic anemometer/thermometer (model CSAT3, Campbell Scientific) and an open-path CH₄ analyzer (model LI-7700, LI-COR, Inc., Lincoln, Nebraska), measures the CH₄

TABLE 2. A list of eddy covariance sites.

Site ID	Site name	Lat/lon	Start date	Water depth (m)	Biology	EC gas analyzer	EC height (m)
DS	Dongshan	31.0799°N/ 120.4346°E	Apr 2011	—	Cropland/ rural residence	Licor 7500	20.0
MLW	Meiliangwan	31.4197°N/ 120.2139°E	Jun 2010	1.8	Eutrophic	Licor 7500A	3.5
DPK	Dapukou	31.2661°N/ 119.9312°E	Aug 2011	2.5	Super eutrophic	Licor 7500	8.5
BFG	Bifenggang	31.1685°N/ 120.3972°E	Dec 2011	1.7	Submerged macrophyte	Campbell EC150	8.5
XLS	Xiaoleishan	30.9972°N/ 120.1344°E	Nov 2012	2.0	Transitional	Campbell EC150	9.4
PTS	Pingtaishan	31.2323°N/ 120.1086°E	Jun 2013	2.8	Mesotrophic	Campbell EC150	8.5

flux. Submerged macrophyte vegetation is abundant in the eddy flux footprint of this site (peak biomass density 1.4 kg m^{-2} ; Liu et al. 2007). These additional measurements will help us to better understand its ecophysiological processes.

All the micrometeorological variables are averaged to half-hourly intervals. The eddy flux and micrometeorological data are retrieved weekly via a cellular communication device (model H7118 GPRS/EDGE DTU, Hongdian Technologies Corporation, Shenzhen, China) and inspected for quality assurance. The 10-Hz EC data are retrieved upon biweekly to monthly site visits. Coordinate rotation into the natural wind system is performed on the EC statistics (Lee et al. 2004) and density corrections are applied to the CO_2 , CH_4 , and H_2O fluxes (Webb et al. 1980).

Lake surveys. To gain a more detailed understanding of spatial variations of the greenhouse gas fluxes, we supplement the eddy covariance measurement with periodic spatial surveys of the concentrations of CO_2 , CH_4 , and N_2O dissolved in the lake water. At monthly intervals, water samples are collected at the 20-cm depth from 17 points across the northern half of the lake. Every three months, water samples are collected from a network of 29 points across the whole lake. The half-lake survey is completed in one day and the whole-lake survey is completed in two consecutive days. The water samples are sealed in 300-mL glass bottles without air space and are analyzed within 24–48 h after collection for the dissolved CO_2 , CH_4 , and N_2O concentrations using the equilibrium method. Pure N_2 gas is injected into the glass bottle, creating a 100-mL headspace. The displaced water is analyzed for alkalinity, pH, and water isotopic compositions. The remaining 200-mL water is then vigorously mixed with the N_2 gas for 5 min to promote liquid–gas equilibrium. The gaseous concentrations of CO_2 , CH_4 , and N_2O are analyzed on a gas chromatography (model 6890N, Agilent Technologies Inc., Loveland, Colorado) and subsequently converted to the dissolved concentration using the Henry law. The water–air flux F is calculated from the bulk diffusion model,

$$F = k(C_b - C_s), \quad (1)$$



FIG. 2. The PTS instrument platform in zone 4 (Fig. 1). Insets are photos of the (left) four-way radiometer and (right) eddy covariance sensors.

where C_s is the CO_2 , CH_4 , or N_2O concentration in equilibrium with ambient air, C_b is the concentration in the bulk water below the interfacial layer, and k is an exchange coefficient (e.g., Cole et al. 1994).

The D and ^{18}O compositions of the water samples are analyzed with isotopic ratio infrared spectroscopy (Model DLT-100, Los Gatos Research). Each sample is measured three times against a working standard traceable to the Vienna Standard Mean Ocean Water (VSMOW) scale. The isotope compositions of the lake water are useful tracer of water currents and provide constraints on the lake evaporative flux.

Modeling lake–air interactions. The modeling component of the project is concerned with science questions 1 and 2. The experimental data are used to improve parameterization of the lake–air interactions. We will test the bulk parameterizations for momentum, sensible heat, and latent heat transfers between the water surface and the atmosphere (Garratt 1992), models of varying complexity for lake evaporation (Brutsaert 1982), and the National Center for Atmospheric Research’s (NCAR’s) 1D diffusion model of heat transfer in lakes (Subin et al. 2012). Another task is to investigate the dynamics of lake–land circulations by embedding these parameterizations in the mesoscale Weather Research and Forecasting (WRF) Model.

EARLY RESULTS. Radiation fluxes. Figure 3 presents an example of the time series of the surface radiation components and the flux variables. The

observation was made in June 2013 over a 10-day period with variable cloudiness. The 24-h mean values for a typical clear-sky day [day of year (DOY) 172 or 21 June 2013] is provided in supplementary Table ES1. The six EC sites track each other very well in terms of the incoming solar radiation (K_{\downarrow}) and the incoming longwave radiation (L_{\downarrow}) despite the large spatial separation among the sites (up to 45 km; Fig. 1), indicating uniform sky conditions across the lake and lack of persistent local disturbance to cloud formation. Among the five lake sites, there are little spatial variations in the outgoing longwave radiation (L_{\uparrow}) except on the clear day (DOY 154) when the BFG site—a site with submerged macrophytes—has a slightly higher value owing to warmer surface water (bottom panel on the right, Fig. 3). The clear-sky albedo shows small but measurable differences among the lake sites: the two eutrophic sites (MLW and DPK) have lower values than the other two cleaner sites (XLS and PTS; see supplementary Table ES1). The macrophyte site (BFG) also has low albedo.

The surface water temperature is surprisingly uniform across the lake, varying by less than 1.5°C among these sites over 90% of the observations shown

in Fig. 3. A notable exception occurred at midday of DOY 154, when the macrophyte site (BFG) was 5.5°C warmer than the rest of the sites. In a sensitivity analysis using the NCAR's lake model, Deng et al. (2013) found that the lake surface temperature is not sensitive to water pollution status or wind speed.

The reflected shortwave radiation (K_{\uparrow}) and the outgoing longwave radiation (L_{\uparrow}) show large land–lake contrasts. On DOY 172, the albedo of the land site (DS) is 0.09–0.11 greater than the lake sites. The outgoing longwave radiation at DS is higher in the day and lower at night than the lake sites. The land surface at DS is warmer in the daytime and cooler at night than the water surface. Generally, the daily mean net radiation is lower at DS than at the lake sites. For example, on DOY174, the net radiation at DS is 174.6 W m⁻² and is 30–40 W m⁻² lower than at the lake sites.

Sensible and latent heat fluxes. The time series plot reveals several features typical of the sensible (H) and latent heat flux (λE) at this lake. Owing to the heat storage in the water column, the fluxes at the lake sites with open fetch (DPK, BFG, XLS, and

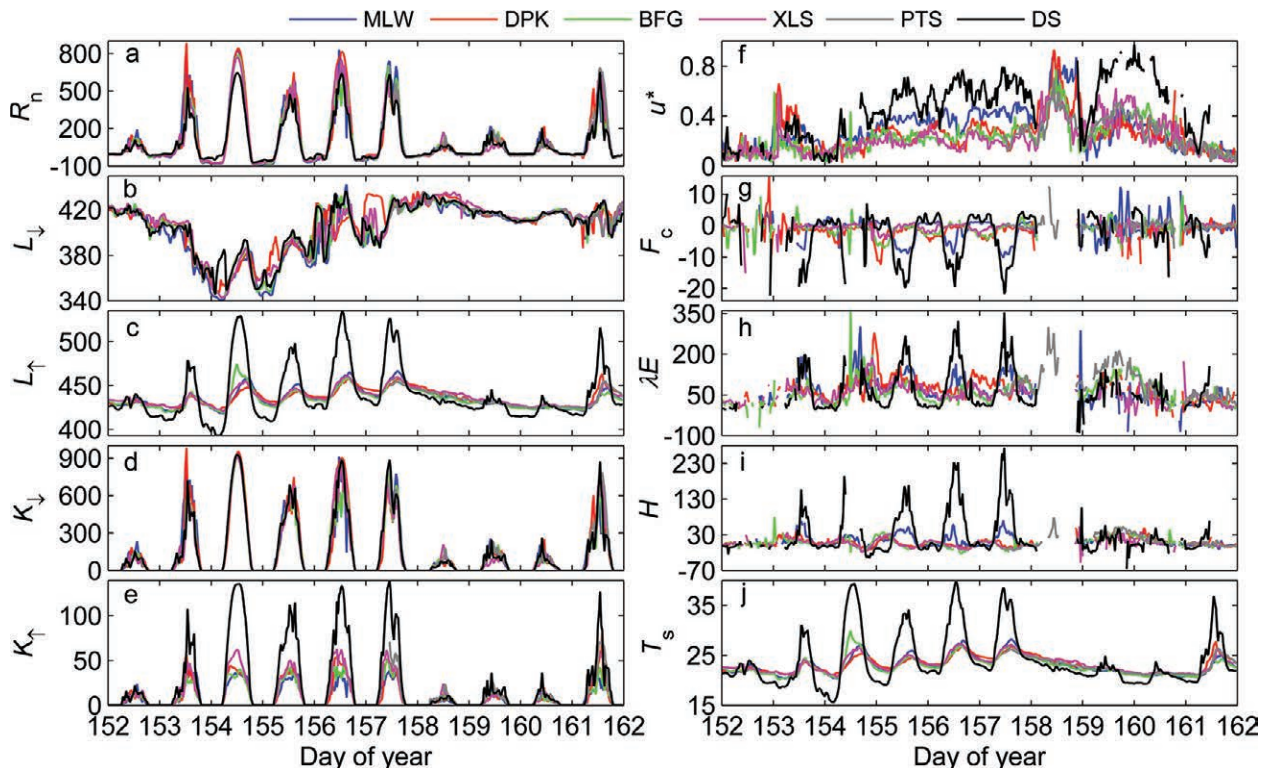


FIG. 3. Time series of micrometeorological and flux variables, DOY 152–162 (1–10 Jun 2013). Ticks on the horizontal axis mark the 00:00 h of the day. Here R_n is net radiation (W m^{-2}), L_{\downarrow} is incoming longwave radiation (W m^{-2}), L_{\uparrow} is outgoing longwave radiation, K_{\downarrow} is incoming shortwave radiation (W m^{-2}), K_{\uparrow} is reflected shortwave radiation (W m^{-2}), u_* is friction velocity (m s^{-1}), F_c is CO_2 flux ($\mu\text{mol m}^{-2} \text{s}^{-1}$), λE is latent heat flux (W m^{-2}), H is sensible heat flux (W m^{-2}), and T_s is surface temperature ($^{\circ}\text{C}$).

PTS) show little diurnal variations. At the MLW site near the north shore, the land influence is evidenced by the large H during a few midday periods (DOY 155–157) when wind blew from the shore. Unlike at Lake Superior where the atmospheric surface layer is generally stable and H is negative during the warm season (Blanken et al. 2011), positive H occurred for about 75% of the observations shown in Fig. 3. The half-hourly H and λE time series at the sites with open fetch track each reasonably well. In Lake Kinneret in a semi-arid climate, spatial variations in evaporation can be as large as 100% on the daily basis (Assouline and Mahrer 1996).

On the monthly time scale, the lake evaporation is controlled primarily by net radiation (Fig. 4a; Wang et al. 2014). When plotted against the available energy, the data collapse onto a single line represented by the Priestley–Taylor evaporation model with the original α coefficient of 1.26, regardless of measurement location in the lake (Fig. 4b). Similar agreement has been reported for a tropical reservoir (dos Reis and Dias 1998). Here we have removed the bias errors of energy imbalance by forcing energy balance closure according to the procedure described by Blanken et al. (1997) and Twine et al. (2000). The data from the land site also follow the Priestley–Taylor model prediction, but with a modified coefficient of 1.0.

Momentum exchange. Unsurprisingly, the friction velocity u_* at the land site (DS) is much higher than at the open-water lake sites (DPK, BFG, XLS, PTS). For the data period shown in Fig. 3, the difference is about a factor of 2. The MLW site has higher friction velocity than the other lake sites, once again a result of land influences. In lake zones sheltered by land vegetation, momentum transfer into the water is usually reduced (Hondzo and Stefan 1993), so the enhanced friction velocity at MLW, measured at the height of 3.5 m above the water, is perhaps more indicative of a wake effect of the land than the true momentum flux from the atmosphere to the water (Markfort et al. 2010). During periods with open fetch (wind direction 200° to 315° ; Fig. 1), however, the MLW drag coefficient is not much different from that at DPK. The drag coefficient is a measure of efficiency of momentum exchange between the lake water and the atmosphere. Under neutral stability it is given as

$$C_{D10N} = \frac{u_*^2}{u_{10}^2},$$

where u_* is friction velocity and u_{10} is wind speed at the 10-m height. According to Xiao et al. (2013), the open-fetch drag coefficient at the wind speed of

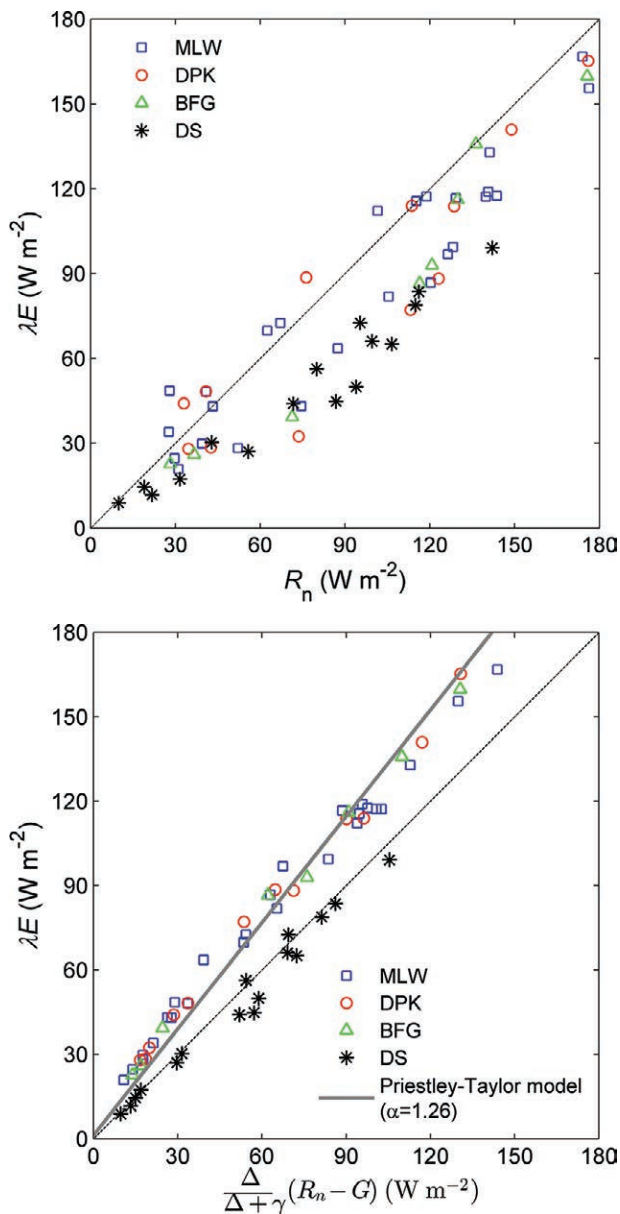


FIG. 4. Monthly latent heat flux λE as a function of (top) net radiation R_n and (bottom) available energy $R_n - G$, where G is heat storage in soil or water, Δ is the slope of the saturation vapor pressure curve, and γ is the psychrometric constant.

$u_{10} = 5 \text{ m s}^{-1}$ is $2.0 (\pm 0.4) \times 10^{-3}$ at DPK, $1.9 (\pm 0.3) \times 10^{-3}$ at MLW, and $1.1 (\pm 0.4) \times 10^{-3}$ at BFG. The BFG site has much lower C_{D10N} because the presence of submerged macrophytes has the effect of reducing the roughness of the water surface. Using the same data analysis method of Xiao et al. (2013), we found that the C_{D10N} values at the other two newer lake sites (XLS and PTS) are also higher than that at BFG ($1.3 \pm 0.4 \times 10^{-3}$ for $u_{10} = 5 \text{ m s}^{-1}$). For comparison, the standard drag coefficient model, established from observations

in the marine environment, predicts a C_{D10N} value of 1.0×10^{-3} at $u_{10} = 5 \text{ m s}^{-1}$ (Garratt 1992).

Carbon dioxide flux. The most interesting feature regarding the CO_2 flux (F_c) data is the negative flux, or CO_2 diffusion into the water, in darkness (DOY 154–157; Fig. 3). These nocturnal uptake events usually persist through the whole evening and have been observed at all the lake sites. They tend to occur in the night following a daylight period of strong solar radiation, although not every high solar radiation day is followed with an uptake event, and are rarely seen under overcast conditions. The nocturnal uptake occurs more frequently at the macrophyte site (BFG), where the plants are totally submerged in water, than

at the other lake sites. In the calendar year 2012, there were 106 night periods with persistent negative flux at BFG and only 76 at DPK. Our results indicate that the macrophyte (*Potamogeton malaianus* and *Hydrilla verticillata*) and phytoplankton species (*Microcystis* and *Navicula*) in Lake Taihu have the capacity to deploy Crassulacean acid metabolism (CAM) for carbon capture (e.g., Maberly and Madsen 2002).

The most negative half-hourly flux ($-24.6 \mu\text{mol m}^{-2} \text{s}^{-1}$) was recorded at BFG on the evening of 30 July (DOY 212; Fig. 5). The flux is too large to be explained by measurement uncertainties; furthermore, the large and persistent nocturnal negative flux caused the CO_2 concentration in the surface air at BFG to reach minima at sunrise as opposed to minima in midafternoon at the site near land (MLW). For comparison, the midday photosynthetic flux of coniferous forests on land is typically $-15 \mu\text{mol m}^{-2} \text{s}^{-1}$ during the growing season (e.g., Goulden et al. 2006), and the nocturnal uptake flux of a land CAM plant is about $-10 \mu\text{mol m}^{-2} \text{s}^{-1}$ following a period of exposure to high photosynthetically active radiation (Nobel and Hartsock 1983). In this latter study, the flux is expressed at the leaf scale as flux density per unit leaf area. In the only published ecosystem-scale carbon flux study involving CAM plants (pineapple), José et al. (2007) reported a nighttime uptake of $-1.1 \mu\text{mol m}^{-2} \text{s}^{-1}$.

The growth of submerged aquatic plants is thought to be diffusion limited (Raven 1970; Smith and Walker 1980; Maberly and Madsen 2002). The molecular diffusivity of CO_2 in water is four orders of magnitude smaller than in air. The leaf boundary layer resistance of plants submerged in stirred water is typically $60\text{--}100 \text{ s cm}^{-1}$ (Black et al. 1981), whereas land plants have a resistance on the order of $0.1\text{--}1 \text{ s cm}^{-1}$ (Campbell 1977). The slow diffusion is also manifested in the small water–air exchange coefficient k . A typical k value for inland lakes is $\sim 0.5 \text{ m day}^{-1}$ (Read et al. 2012), which would cap the CO_2 uptake at no more than $\sim 0.1 \mu\text{mol m}^{-2} \text{s}^{-1}$ according to Eq. (1). The negative F_c values in this study exceed the diffusion limit by two orders of magnitude, calling into question the applicability of the diffusion limitation paradigm at this shallow lake.

The uptake events start precisely at the time when ΔT_w switches from being negative to being positive in the late afternoon and end when ΔT_w turns negative again the next morning (Fig. 5). Here ΔT_w is the difference in water temperature between the 100- and the 20-cm depth. At this lake, water temperature is almost always greater than 4°C , so a positive ΔT_w is indicative of convective instability of the water

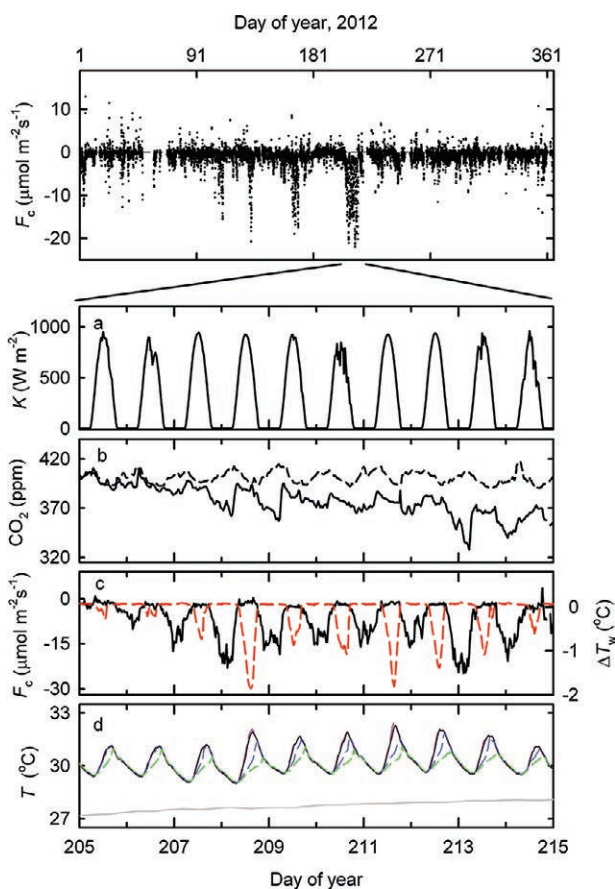


FIG. 5. (top) Half-hourly CO_2 flux at BFG. (bottom) Half-hourly time series for a 10-day period (23 Jul–1 Aug 2012). (a) Incoming shortwave radiation at BFG, (b) CO_2 mixing ratio at BFG (solid line) and at MLW (dashed line), (c) CO_2 flux (black solid line) and 0.2–1.0-m water temperature difference ΔT_w (1.0-m temperature minus 0.2-m temperature; red dashed line) at BFG, and (d) water (purple dashed line, 0.2 cm; solid black line, 0.5 m; blue dashed line, 1 m; green dashed line, 1.5 m) and sediment temperature (gray line) at BFG.

column. It appears that the bulk diffusion model [Eq. (1)] needs serious revision under conditions of convective instability and in the presence of an active sink in the water column.

The CAM of aquatic plants is hypothesized to be an adaptation to diffusion limitation (Maberly and Madsen 2002). Our alternative hypothesis is that in shallow lakes, diffusion is not a limiting factor during most nights because of convective instability in the water column, and CAM is a physiological mechanism adapted to the high availability of the CO_2 resource at night.

Spatial patterns from lake surveys.

Figure 6 presents an example of the data collected during a whole-lake survey. This and other surveys reveal spatially coherent patterns in the dissolved CO_2 , CH_4 , and N_2O concentrations and in the water $^{18}\text{O}/^{16}\text{O}$ isotopic ratio. During this survey, which took place on 13–14 May 2013 between 0600 and 1630 local time, the mean lake water temperature is 22.1°C . For reference, the gas concentration in equilibrium with the ambient air is $16.3 \mu\text{mol L}^{-1}$ (CO_2), 2.9 nmol L^{-1} (CH_4), and 9.4 nmol L^{-1} (N_2O). The mean (± 1 standard deviation) of the dissolved CO_2 concentration is 36.4 (± 29.5) $\mu\text{mol L}^{-1}$. Of the 29 sampling locations, 27 are supersaturated, having CO_2 concentration values greater than the equilibrium value. The highest values were observed in zone 3 (Fig. 1), indicating the dominant role of river carbon import.

The mean N_2O concentration is $13.3 \pm 9.4 \text{ nmol L}^{-1}$, with the majority of the sampling locations (22) being supersaturated with respect to the atmosphere. The N_2O concentration shows a northwest to southeast gradient with the highest values observed in zone 3 (Fig. 6c). This pattern is similar to that of CO_2 (Fig. 6a) and also resembles the spatial variations of the total N concentration reported for the lake (Yan et al. 2011).

In contrast to CO_2 and N_2O , the highest CH_4 concentrations were observed in zones 5 and 7 dominated by macrophyte habitats (Fig. 6b). We interpret this as evidence that the main source of CH_4 in this lake is the organic carbon from the primary production of macrophyte plants. All the sampling sites are supersaturated in CH_4 with respect to the atmosphere, with the mean concentration of $94.2 \pm 120.1 \text{ nmol L}^{-1}$.

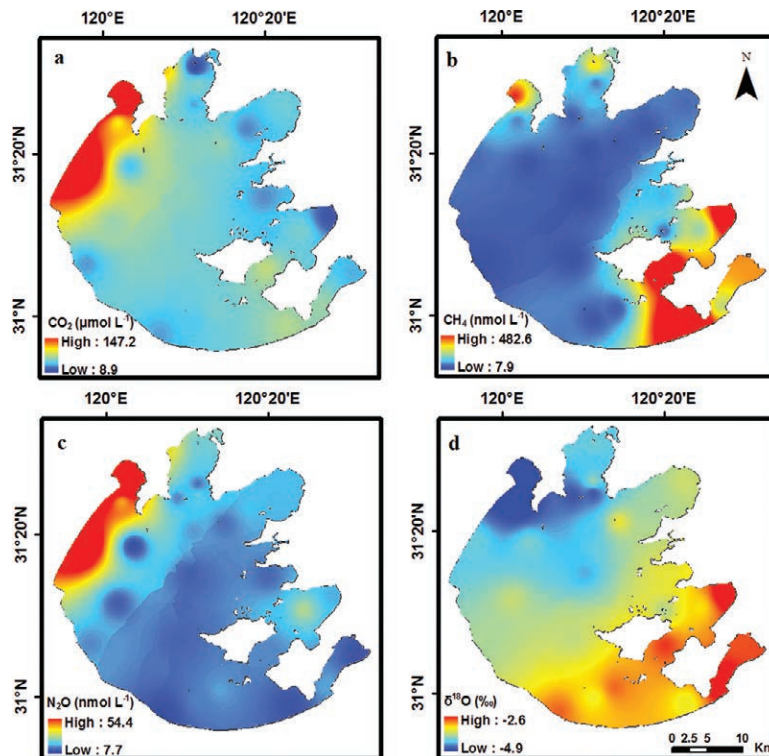


FIG. 6. Spatial distributions of dissolved (a) CO_2 , (b) CH_4 , and (c) N_2O concentration and (d) the ^{18}O composition of the lake water, 13–14 May 2013.

Among the three gas species measured, CH_4 shows the largest spatial variations: the ratio of the maximum to minimum concentration is 61. For comparison, the maximum-to-minimum concentration ratio is 17 for CO_2 and 7 for N_2O .

The ^{18}O composition of the lake water becomes progressively enriched from north to south (Fig. 6d). The mean value for the whole lake is -3.71 ± 0.52 per mil (VSMOW scale) and is closer to the ^{18}O composition of the outflows (-3.88 ± 0.87 per mil) than that of the inflows (-5.08 ± 0.86 per mil), both of which were measured on 21–22 May 2013. The enrichment, caused by the kinetic and equilibrium fractionation during evaporation, can be viewed as a proxy for “water age” or the time elapsed since the water enters the lake via the inflow rivers and precipitation. It appears that at this time of the year, the lake water moved predominantly in the north–south direction.

Modeling lake–air interactions. The data collected at Lake Taihu have been used to improve the lake model in NCAR’s Community Land Model (CLM) system. In the latest version of the CLM lake model (Subin et al. 2012), the water column is divided into 10 layers, and heat diffusion between the adjacent layers is described by a one-dimensional diffusion equation.

Tests of the model for deep lakes reveal that the eddy thermal diffusivity given by the model is 1–2 orders of magnitude too low (Martynov et al. 2010; Subin et al. 2012). In contrast, we found that for Lake Taihu the diffusivity should be adjusted downward by 92% in order for the model to reproduce successfully the observed diurnal variations in the lake surface temperature (Deng et al. 2013). The small eddy diffusivity suggests that unresolved vertical eddy motions are weak or absent at this large and shallow lake.

The tuned lake model has now been successfully coupled to the WRF Model. In the default version of WRF V3.3.1, the lake surface temperature is set to the sea surface temperature at the same latitude and the surface sensible and latent heat fluxes are computed with a bulk scheme. The tuned lake model shows significant improvement over the WRF default in the predictions of the surface state and flux variables (see Fig. ES2 and Table ES2 in the online supplement). These improvements should lead to more realistic simulations of the lake breeze circulation.

SUMMARY. The experimental objective of this field program is to quantify the lake–air fluxes of energy, momentum, and greenhouse gases across pollution and biological gradients in the lake. The data collected so far indicate that (i) the radiation balance components and surface temperature show very small variations across the lake, (ii) the momentum exchange is reduced at the habitat of submerged macrophytes, (iii) there is evidence of CAM for carbon capture, and (iv) there are large spatial gradients of the concentrations of CO₂, CH₄, and N₂O dissolved in the lake water. The ongoing field experiment, data analysis, and model development will attempt to answer the five science questions outlined in section 1.

ACKNOWLEDGMENTS. This research was supported by the Ministry of Education of China (Grant PCSIRT), the Priority Academic Program Development of Jiangsu Higher Education Institutions (Grant PAPD), the National Science Foundation of China (Grant 41275024), and the Natural Science Foundation of Jiangsu Province, China (Grant BK2010572). We thank Prof. Peter Raymond of Yale University and Prof. Shuqing An of Nanjing University for helpful discussions and Dr. David Fitzjarrald and two anonymous reviewers for their constructive comments on this paper.

REFERENCES

An, S., and R. Wang, 2008: Human-induced drivers of the development of Lake Taihu. *Lectures on China's Environment*, X. Lee, Ed., Yale School of Forestry

and Environmental Studies Publication Series, Vol. 20, 151–165.

- Assouline, S., and Y. Mahrer, 1996: Spatial and temporal variability in microclimate and evaporation over Lake Kinneret: Experimental evaluation. *J. Appl. Meteor.*, **35**, 1076–1084, doi:10.1175/1520-0450(1996)035<1076:SATVIM>2.0.CO;2.
- Baldocchi, D., and Coauthors, 2001: FLUXNET: A new tool to study the temporal and spatial variability of ecosystem-scale carbon dioxide, water vapor, and energy flux densities. *Bull. Amer. Meteor. Soc.*, **82**, 2415–2434, doi:10.1175/1520-0477(2001)082<2415:FANTTS>2.3.CO;2.
- Balmer, M. B., and J. A. Downing, 2011: Carbon dioxide concentrations in eutrophic lakes: Undersaturation implies atmospheric uptake. *Inland Waters*, **1**, 125–132, doi:10.5268/IW-1.2.366.
- Bastviken, D., L. J. Tranvik, J. A. Downing, P. M. Crill, and A. Enrich-Prast, 2011: Freshwater methane emissions offset the continental carbon sink. *Science*, **331**, 50, doi:10.1126/science.1196808.
- Black, M. A., S. C. Maberly, and D. H. N. Spence, 1981: Resistances to carbon dioxide fixation in four submerged freshwater macrophytes. *New Phytol.*, **89**, 557–568, doi:10.1111/j.1469-8137.1981.tb02335.x.
- Blanken, P. D., and Coauthors, 1997: Energy balance and canopy conductance of a boreal aspen forest: Partitioning overstory and understory components. *J. Geophys. Res.*, **102**, 28 915–28 927, doi:10.1029/97JD00193.
- , and Coauthors, 2011: Evaporation from Lake Superior: 1. Physical controls and processes. *J. Great Lakes Res.*, **37**, 707–716
- Brown, M. G., and Coauthors, 2012: The carbon balance of two lodgepole pine stands recovering from mountain pine beetle attack in British Columbia. *Agric. For. Meteorol.*, **153**, 82–93, doi:10.1016/j.agrformet.2011.07.010.
- Brutsaert, W. H., 1982: *Evaporation into the Atmosphere*. D. Reidel, 299 pp.
- Campbell, G. S., 1977: *Introduction to Environmental Biophysics*. Springer, 159 pp.
- Cole, J. J., and N. F. Caraco, G. W. Kling, and T. K. Kratz, 1994: Carbon dioxide supersaturation in the surface waters of lakes. *Science*, **265**, 1568–1570.
- Deng, B., S. Liu, W. Xiao, W. Wang, J. Jin, and X. Lee, 2013: Evaluation of the CLM4 lake model at a large and shallow freshwater lake. *J. Hydrometeorol.*, **14**, 636–649, doi:10.1175/JHM-D-12-067.1.
- dos Reis, R. J., and N. L. Dias, 1998: Multi-season lake evaporation: Energy-budget estimates and CRLE model assessment with limited meteorological observations. *J. Hydrol.*, **208**, 135–147, doi:10.1016/S0022-1694(98)00160-7.

- Downing, J. A., and Coauthors, 2006: The global abundance and size distribution of lakes, ponds, and impoundments. *Limnol. Oceanogr.*, **51**, 2388–2397, doi:10.4319/lo.2006.51.5.2388.
- Garratt, J. R., 1992: *The Atmospheric Boundary Layer*. Cambridge University Press, 316 pp.
- Goulden, M. L., and Coauthors, 2006: An eddy covariance mesonet to measure the effect of forest age on land-atmosphere exchange. *Global Change Biol.*, **12**, 2146–2162, doi:10.1111/j.1365-2486.2006.01251.x.
- Hari, P., J. Pumpanen, J. Huotari, P. Kolari, J. Grace, T. Vesala, and A. Ojala, 2008: High-frequency measurements of productivity of planktonic algae using rugged nondispersive infrared carbon dioxide probes. *Limnol. Oceanogr. Methods*, **6**, 347–354, doi:10.4319/lom.2008.6.347.
- Hondzo, M., and H. G. Stefan, 1993: Lake water temperature simulation model. *J. Hydraul. Eng.*, **119**, 1251–1273, doi:10.1061/(ASCE)0733-9429(1993)119:11(1251).
- Hu, W., S. E. Jørgensen, F. Zhang, Y. Chen, Z. Hu, and L. Yang, 2011: A model on the carbon cycling in Lake Taihu, China. *Ecol. Modell.*, **222**, 2973–2991, doi:10.1016/j.ecolmodel.2011.04.018.
- Huttunen, J. T., and Coauthors, 2003: Fluxes of methane, carbon dioxide and nitrous oxide in boreal lakes and potential anthropogenic effects on the aquatic greenhouse gas emissions. *Chemosphere*, **52**, 609–621, doi:10.1016/S0045-6535(03)00243-1.
- José, J. S., R. Montes, and N. Nikonova, 2007: Seasonal patterns of carbon dioxide, water vapour and energy fluxes in pineapple. *Agric. For. Meteorol.*, **147**, 16–34, doi:10.1016/j.agrformet.2007.06.003.
- Lee, X., W. Massman, and B. Law, 2004: *Handbook of Micrometeorology: A Guide for Surface Flux Measurement and Analysis*. Kluwer Academic, 250 pp.
- Liu, H., Q. Zhang, and G. Dowler, 2012: Environmental controls on the surface energy budget over a large southern inland water in the United States: An analysis of one-year eddy covariance flux data. *J. Hydrometeorol.*, **13**, 1893–1910, doi:10.1175/JHM-D-12-020.1.
- Liu, W., W. Hu, Y. Chen, X. Gu, Z. Hu, Y. Chen, and J. Ji, 2007: Temporal and spatial variation of aquatic macrophytes in West Taihu Lake. *Acta Ecol. Sin.*, **27**, 159–170.
- Maberly, S. C., and T. V. Madsen, 2002: Freshwater angiosperm carbon concentrating mechanisms: Processes and patterns. *Funct. Plant Biol.*, **29**, 393–405, doi:10.1071/PP01187.
- Markfort, C. D., A. L. S. Perez, J. W. Thill, D. A. Jaster, F. Porté-Agel, and H. G. Stefan, 2010: Wind sheltering of a lake by a tree canopy or bluff topography. *Water Resour. Res.*, **46**, W03530, doi:10.1029/2009WR007759.
- Martynov, A., L. Sushama, and R. Laprise, 2010: Simulation of temperate freezing lakes by one-dimensional lake models: Performance assessment for interactive coupling with regional climate models. *Boreal Environ. Res.*, **15**, 143–164.
- Nobel, P. S., and T. L. Hartssock, 1983: Relationships between photosynthetically active radiation, nocturnal acid accumulation, and CO₂ uptake for a Crassulacean acid metabolism plant, *Opuntia ficus-indica*. *Plant Physiol.*, **71**, 71–75, doi:10.1104/pp.71.1.71.
- Nordbo, A., S. Launiainen, I. Mammarella, M. Leppäranta, J. Huotari, A. Ojala, and T. Vesala, 2011: Long-term energy flux measurements and energy balance over a small boreal lake using eddy covariance technique. *J. Geophys. Res.*, **116**, D02119, doi:10.1029/2010JD014542.
- Prescher, A. K., T. Grunwald, and C. Bernhofer, 2010: Land use regulates carbon budgets in eastern Germany: From NEE to NBP. *Agric. For. Meteorol.*, **150**, 1016–1025, doi:10.1016/j.agrformet.2010.03.008.
- Qin, Q., P. Xu, Q. Wu, L. Luo, and Y. Zhang, 2007: Environmental issues of Lake Taihu, China. *Hydrobiologia*, **581**, 3–14, doi:10.1007/s10750-006-0521-5.
- Raven, J. A., 1970: Exogenous inorganic carbon sources in plant photosynthesis. *Biol. Rev. Camb. Philos. Soc.*, **45**, 167–221, doi:10.1111/j.1469-185X.1970.tb01629.x.
- Read, J. S., and Coauthors, 2012: Lake-size dependency of wind shear and convection as controls on gas exchange. *Geophys. Res. Lett.*, **39**, L09405, doi:10.1029/2012GL051886.
- Rouse, W. R., P. D. Blanken, N. Bussièrès, C. J. Oswald, W. M. Schertzer, C. Spence, and A. E. Walker, 2008: Investigation of the thermal and energy balance regimes of Great Slave and Great Bear Lakes. *J. Hydrometeorol.*, **9**, 1318–1333, doi:10.1175/2008JHM977.1.
- Samuelsson, P., E. Kourzeneva, and D. Mironov, 2010: The impact of lakes on the European climate as simulated by a regional climate model. *Boreal Environ. Res.*, **15**, 113–129.
- Schimel, D., W. Hargrove, F. Hoffman, and J. MacMahon, 2007: NEON: A hierarchically designed national ecological network. *Front. Ecol. Environ.*, **5**, 59, doi:10.1890/1540-9295(2007)5[59:NAHDNE]2.0.CO;2.
- Schubert, C. J., T. Diem, and W. Eugster, 2012: Methane emissions from a small wind shielded lake determined by eddy covariance, flux chambers, anchored funnels, and boundary model calculations: A comparison. *Environ. Sci. Technol.*, **46**, 4515–4522, doi:10.1021/es203465x.

- Sills, D. M. L., J. R. Brook, I. Levy, P. A. Makar, J. Zhang, and P. A. Taylor, 2011: Lake breezes in the southern Great Lakes region and their influence during BAQS-Met 2007. *Atmos. Chem. Phys.*, **11**, 7955–7973, doi:10.5194/acp-11-7955-2011.
- Smith, F. A., and N. A. Walker, 1980: Photosynthesis by aquatic plants: Effects of unstirred layers in relation to assimilation of CO₂ and HCO₃ and to carbon isotope discrimination. *New Phytol.*, **86**, 245–259, doi:10.1111/j.1469-8137.1980.tb00785.x.
- St. Louis, V. L., C. A. Kelly, É. Duchemin, J. W. M. Rudd, and D. M. Rosenberg, 2000: Reservoir surfaces as sources of greenhouse gases to the atmosphere: A global estimate. *Bioscience*, **50**, 766–775, doi:10.1641/0006-3568(2000)050[0766:RSASOG]2.0.CO;2.
- Stoy, P. C., G. G. Katul, M. B. S. Siqueira, J. Y. Juang, K. A. Novick, H. R. McCarthy, A. C. Oishi, and R. Oren, 2008: Role of vegetation in determining carbon sequestration along ecological succession in the southeastern United States. *Global Change Biol.*, **14**, 1409–1427, doi:10.1111/j.1365-2486.2008.01587.x.
- Subin, Z. M., W. J. Riley, and D. V. Mironov, 2012: An improved lake model for climate simulations: Model structure, evaluation, and sensitivity analyses in CESM1. *J. Adv. Model. Earth Syst.*, **4**, M02001, doi:10.1029/2011MS000072.
- Taihu Office, 2012: *The 2013 Health Report of Lake Taihu*. Taihu Bureau, Ministry of Water Resources of China, Shanghai Office, 16 pp.
- Twine, T. E., and Coauthors, 2000: Correcting eddy-covariance flux underestimates over a grassland. *Agric. For. Meteorol.*, **103**, 279–300, doi:10.1016/S0168-1923(00)00123-4.
- Wang, W., and Coauthors, 2014: Temporal and spatial variations in radiation and energy balance across a large freshwater lake in China. *J. Hydrol.*, **511**, 811–824, doi:10.1016/j.jhydrol.2014.02.012.
- Webb, E. K., G. I. Pearman, and R. Leuning, 1980: Correction of flux measurements for density effects due to heat and water vapor transfer. *Quart. J. Roy. Meteor. Soc.*, **106**, 85–100, doi:10.1002/qj.49710644707.
- Xiao, W., S. Liu, W. Wang, D. Yang, J. Xu, C. Cao, H. Li, and X. Lee, 2013: Transfer coefficients of momentum, heat and water vapour in the atmospheric surface layer of a large freshwater lake. *Bound.-Layer Meteorol.*, **148**, 479–494, doi:10.1007/s10546-013-9827-9.
- Yan, S., H. Yu, L. Zhang, J. Xu, and Z. Wang, 2011: Water quantity and pollutant fluxes of inflow and outflow rivers of Lake Taihu 2009. *J. Lake Sci.*, **23**, 855–862.
- Zha, T., and Coauthors, 2009: Carbon sequestration in boreal jack pine stands following harvesting. *Global Change Biol.*, **15**, 1475–1487, doi:10.1111/j.1365-2486.2008.01817.x.
- Zhang, X., and Coauthors, 2010: The 2007 water crisis in Wuxi, China: Analysis of the origin. *J. Hazard. Mater.*, **182**, 130–135, doi:10.1016/j.jhazmat.2010.06.006.
- Zhao, G., J. Gao, P. Tian, K. Tian, and G. Ni, 2011: Spatial-temporal characteristics of surface water quality in the Taihu Basin, China. *Environ. Earth Sci.*, **64**, 809–819, doi:10.1007/s12665-011-0902-6.
- Zhao, L., J. Jin, S. Y. Wang, and M. B. Ek, 2012: Integration of remote-sensing data with WRF to improve lake-effect precipitation simulations over the Great Lakes region. *J. Geophys. Res.*, **117**, D09102, doi:10.1029/2011JD016979.

THE TAIHU EDDY FLUX NETWORK

An Observational Program on Energy, Water, and Greenhouse Gas Fluxes of a Large Freshwater Lake

BY XUHUI LEE, SHOUDONG LIU, WEI XIAO, WEI WANG, ZHIQIU GAO, CHANG CAO, CHENG HU, ZHENGHUA HU, SHUANGHE SHEN, YONGWEI WANG, XUEFA WEN, QITAO XIAO, JIAPING XU, JINBIAO YANG, AND MI ZHANG

This document is a supplement to “The Taihu Eddy Flux Network: An Observational Program on Energy, Water, and Greenhouse Gas Fluxes of a Large Freshwater Lake,” by Xuhui Lee, Shoudong Liu, Wei Xiao, Wei Wang, Zhiqiu Gao, Chang Cao, Cheng Hu, Zhenghua Hu, Shuanghe Shen, Yongwei Wang, Xuefa Wen, Qitao Xiao, Jiaping Xu, Jinbiao Yang, and Mi Zhang (*Bull. Amer. Meteor. Soc.*, **95**, 1583–1594) • ©2014 American Meteorological Society • Corresponding author: Xuhui Lee, School of Forestry and Environmental Studies, Yale University, New Haven, CT 06511 • E-mail: xuhui.lee@yale.edu • DOI: 10.1175/BAMS-D-13-00136.2

TABLE ES1. Daily mean values of micrometeorological and flux variables, 21 Jun (DOY 172) 2013. Here T_a is air temperature ($^{\circ}\text{C}$), T_s is surface temperature ($^{\circ}\text{C}$), T_{100} is water temperature at the 100-cm depth ($^{\circ}\text{C}$), U_{10} is wind speed at the 10-m height above the water (m s^{-1}), RH is relative humidity (%), K_{\downarrow} is incoming shortwave radiation (W m^{-2}), K_{\uparrow} is reflected shortwave radiation (W m^{-2}), L_{\downarrow} is incoming longwave radiation (W m^{-2}), L_{\uparrow} is outgoing longwave radiation (W m^{-2}), α is albedo (dimensionless), R_n is net all-wave radiation (W m^{-2}), u_* is friction velocity (m s^{-1}), H is sensible heat flux, λE is latent heat flux, β is the Bowen ratio (dimensionless), and F_c is CO_2 flux ($\text{mg m}^{-2} \text{s}^{-1}$).

Site ID	DS	MLW	DPK	BFG	XLS	PTS
T_a	25.7	25.6	25.9	26.0	25.8	25.9
T_s	28.8	27.9	27.8	28.1	28.1	26.7
T_{100}	—	27.7	28.0	27.1	27.8	27.1
U_{10}	2.6	2.4	3.8	3.5	3.3	4.4
RH	65.2	64.2	65.0	72.5	73.9	74.7
K_{\downarrow}	292.3	287.1	290.1	286.8	285.3	296.0
K_{\uparrow}	48.3	15.8	15.1	15.2	19.0	23.2
L_{\downarrow}	399.9	399.4	404.5	401.2	399.9	399.7
L_{\uparrow}	469.3	463.8	463.6	465.0	465.3	456.9
α	0.165	0.055	0.052	0.053	0.067	0.078
R_n	174.6	206.8	215.9	207.8	200.9	215.6
u_*	0.31	0.23	0.24	0.16	0.15	0.17
H	50.2	21.5	13.0	9.5	12.8	8.5
λE	109.4	112.0	146.6	100.0	115.8	117.2
β	0.46	0.19	0.09	0.09	0.11	0.07
F_c	-0.155	-0.072	-0.057	-0.044	-0.011	-0.040

TABLE S2. Linear correlation coefficient between modeled and observed variables: R1 is the correlation for WRF with default lake parameterization, R2 is the correlation for WRF with tuned CLM parameterization, T_s is surface temperature, T_{2m} is 2-m air temperature, R_n is net radiation, H is sensible heat flux, λE is latent heat flux, and G is heat storage.

	T_s	T_{2m}	R_n	H	λE	G
R1	-0.19	0.67	0.90	0.51	0.21	—
R2	0.92	0.83	0.90	0.57	0.58	0.91



FIG. ES1. Water sample taken in zone 3, near the eddy covariance site DPK (Fig. 1).

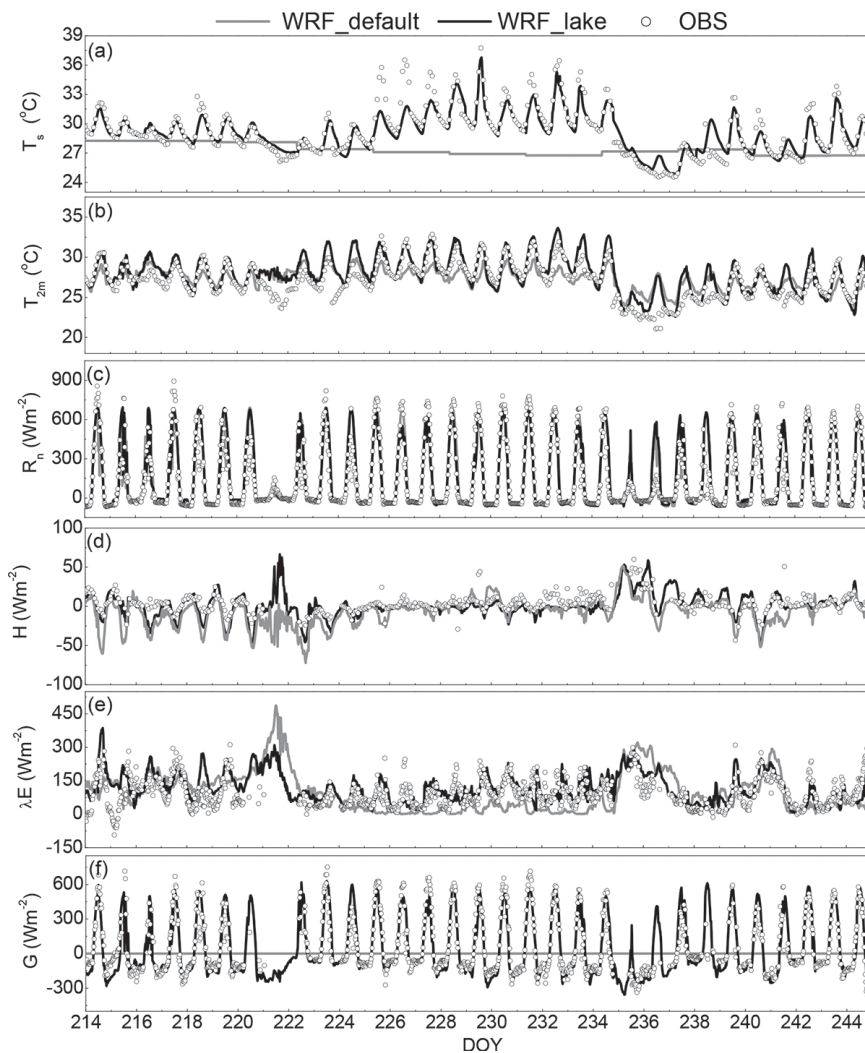


FIG. ES2. Comparison of WRF-predicted surface flux and state variables against the observations at the BFG lake site in Aug 2012. Open circles denote observations, gray line denotes WRF with default lake parameterization, and black line denotes WRF with tuned CLM lake model. Here T_s is surface temperature, T_{2m} is 2-m air temperature, R_n is net radiation, H is sensible heat flux, λE is latent heat flux, and G is heat storage.